Cancer Chemother Pharmacol (2002) 49: 35–47
DOI 10.1007/s00280-001-0388-0

ORIGINAL ARTICLE

**Tsugitaka Natsume · Yasuhiro Koh
Motohiro Kobayashi · Hisao Fukumoto
Fumiyuki Takahashi · Takashi Nakamura
Yuichiro Ohe · Nagahiro Saijo · Kazuto Nishio**

Enhanced antitumor activities of TZT-1027 against TNF-α or IL-6 secreting Lewis lung carcinoma in vivo

Received: 25 March 2001 / Accepted: 31 August 2001 / Published online: 16 November 2001

Abstract *Purpose*: TZT-1027, an antimicrotubule agent that inhibits the polymerization of tubulin, shows potent antitumor activity in various transplantable tumor models in vivo. The high antitumor activity of TZT-1027 prompted us to speculate that this compound may have a mode of action other than its antimicrotubule and antimitotic activities. To elucidate the interaction of antitumor cytokines with TZT-1027 in tumors in vivo, we examined the antitumor activity of this agent against various cytokine gene-transfected Lewis lung carcinoma (LLC) cells inoculated into C57BL/6 mice. *Methods*: In vitro growth inhibition was evaluated using the MTT assay, and in vivo activity was evaluated in subcutaneous models in C57BL/6 mice. The status of the vasculature in tumor tissues was evaluated immunohistochemically using anti-CD31 antibody. We used a cDNA macroarray to examine the gene expression profiles in tumor tissues removed from mice. *Results*: TZT-1027 at 3 mg/kg showed potent antitumor activity in Mock (LLC-Neo cells) inoculated mice with a T/C% value of 16%. TZT-1027 at 3 mg/kg showed more potent antitumor activity in LLC-TNF cells and LLC-IL6 cells with T/C% values of 4% and 3%, respectively. TZT-1027 treatment destroyed the tumor vasculature as well as tumor cells in LLC-TNF and LLC-IL6 tissues of mice treated with TZT-1027. The LLC-TNF and LLC-IL6 tissues of mice treated with TZT-1027 had in common the independent alteration of the non-histone chromosomal protein HMG-14 and transcription factor 1 for heat shock gene. Focusing on the gene regulation related to angiogenesis, the alteration in transcriptional factors such as ets family genes and homeobox family genes was remarkable. *Conclusions*: These factors are candidates as determinants of the enhanced TZT-1027 antitumor activity in relation to these cytokines.

Keywords TZT-1027 · TNF-α · IL-6 · Angiogenesis · Macroarray

T. Natsume · M. Kobayashi
Pharmacological Research Department,
Teikoku Hormone Mfg., Co. Ltd., 1604 Shimosakunobe,
Takatsu-ku, Kawasaki-shi, Kanagawa 213-8522, Japan

Y. Koh · H. Fukumoto · F. Takahashi
T. Nakamura · K. Nishio (✉)
Pharmacology Division,
National Cancer Center Research Institute,
5-1-1 Tsukiji, Chuo-ku, Tokyo 104-0045, Japan
E-mail: knishio@gan2.ncc.go.jp
Tel.: +81-3-35422511
Fax: +81-3-35421886

Y. Ohe · N. Saijo
Medical Oncology, National Cancer Center Hospital,
5-1-1 Tsukiji, Chuo-ku, Tokyo 104-0045, Japan

Introduction

TZT-1027, a novel antimicrotubule agent, is a dolastatin 10 derivative designed to have enhanced antitumor activity and reduced toxicity [31]. The chemical structure of TZT-1027 is shown in Fig. 1. Administration of TZT-1027 to mice by intravenous (i.v.) injection has been shown to markedly inhibit the growth of P388 leukemia and three solid tumors, and TZT-1027 has also been shown to be effective against human tumor xenografts [23]. Pharmacological research has demonstrated that TZT-1027 in the 1–10 μ*M* concentration range inhibits the polymerization of microtubule protein with an IC_{50} of 2.2 μ*M* [23] and monosodium glutamate-induced tubulin polymerization with an IC_{50} of 1.2 μ*M* [36]. Mitotic arrest occurs in TZT-1027-treated cells with the observation of Bcl-2 phosphorylation and apoptosis [52]. However, the exact relationship between the actions of TZT-1027 against microtubules and its antitumor effects has not been clarified in detail in vivo. TZT-1027 is currently undergoing clinical evaluation.

Cytokine gene-transfected Lewis lung carcinoma (LLC) cell lines have been used as an in vitro model to assess cytokine gene therapy in initial clinical studies [16, 17, 40, 41, 42]. They were developed using the plasmid pBMG (eukaryotic cDNA expression vector BMG Neo) and transfected into LLC cells [16, 17, 40, 41, 42]. These

cells were transplanted subcutaneously into and were able to grow in C57BL/6 mice [16, 17, 40, 41, 42].

Some antimicrotubule agents have an effect on tumor vasculature [2, 9, 11, 18, 19, 39]. TZT-1027 at doses of 2 or 3 mg/kg induces scab formation and hemorrhagic necrosis in colon 26 adenocarcinoma (unpublished data). This is similar to the effects of TNF-α induction [47]. Furthermore, TZT-1027 shows potent antitumor activity against cytokine-secreting colon 26 adenocarcinoma via tumoral vascular collapse and tumor cell death [44]. Relationships between the cytokines and tumor vasculature have been reported by several investigators. Some cytokines such as TNF-α and IL-6 induce angiogenesis and tumor vascular disruption [13, 15, 28, 30, 43, 45, 46]. Therefore, this study was designed to elucidate the interactions among cytokines, TZT-1027 and the antitumor properties associated with the effects on tumor vasculature. In addition, we examined the gene expression profiles of tumors inoculated into C57BL/6 mice treated with TZT-1027 for 24 h using the cDNA expression array technique in order to identify candidate molecules possibly involved in the enhanced antitumor activity of TZT-1027 in these cytokine-expressing tumors.

Materials and methods

Reagents

TZT-1027 was synthesized in the laboratories of Teikoku Hormone Mfg. Co., Ltd. (Kawasaki, Japan). TZT-1027 was dissolved in and diluted with 0.05 *M* lactate buffer. Dilution from 1 mg/ml stock solution was performed on each day of the experiment. MTT [3-(4,5-dimethythiazol-2-yl)-2,5-diphenyl-tetrazolium bromide] was obtained from Sigma Chemical Co. (St. Louis, Mo.). Rat anti-mouse CD31 (PECAM-1) antibody was purchased from Pharmingen (Tokyo, Japan) and a Vectastain ABC Elite kit from Vector Laboratories (Burlingame, Calif.). The Atlas Mouse cancer cDNA expression array was obtained from Clontech Laboratories (Palo Alto, Calif.). [α-^{32}P]dATP (3000 Ci/mmol) was purchased from NEN Life Science Products (Boston, Mass.).

Cell lines and experimental animals

LLC cells originated as a spontaneous carcinoma of the lung in a C57BL/6 mouse [29, 49]. LLC cells and transfectant cells were cultured in Iscove's modified minimum essential medium (GIBCO BRL, Gaithersburg, Md.) with 20% FCS (GIBCO BRL) at 37°C in humidified air containing 5% CO_2. Female C57BL/6 mice at 5 weeks of age were purchased from Japan Charles River Company (Atsugi, Japan) and were maintained under specific pathogen-free conditions in our laboratory.

Cytokine cDNA transfectants

LLC cells were transfected with BMG Neo, BMG Neo-TNF, BMG Neo-GM-CSF, BMG Neo-IL2, BMG Neo-IL6 and BMG Neo-IGIF as described elsewhere [14, 16, 17, 21, 40, 41, 42]. The cells were cultured in Iscove's modified minimum essential medium containing 1 mg/ml G418 for selection.

MTT assay

The cell growth-inhibitory effects of TZT-1027 on the various cytokine gene-transfected LLC cell lines in vitro were determined using the MTT assay according to the method of Mosmann [34]. Briefly, cells were harvested in 96-well microplates in a volume of 180 μl and incubated for 24 h at 37°C in humidified air containing 5% CO_2. TZT-1027 was added to individual wells in a volume of 20 μl, and the cells were incubated for 72 h at 37°C in humidified air containing 5% CO_2. MTT reagents were then added to each well in a volume of 20 μl, and the cells were incubated for 4 h at 37°C in humidified air containing 5% CO_2. Finally, the growth inhibitory effect of TZT-1027 was assessed spectrophotometrically (BIO-TEK Instruments, Vt.).

In vivo evaluation of tumor growth

The transfected LLC cells were harvested during exponential growth. Cells were washed twice in Hanks' solution (GIBCO BRL, Gaithersburg, Md.) and 10^6 cells of each cytokine gene-transfected LLC line except for 3×10^6 cells of LLC-TNF cells were injected subcutaneously into the right flank of C57BL/6 mice. The LLC-IL2 cells were rejected due to a host-immune response after inoculation. Therefore, LLC cells were inoculated into the right flank of C57BL/6 mice and, simultaneously, LLC-IL2 cells were injected into the left flank in order to evaluate the effects of IL-2 [41]. IL-2 secreted from LLC-IL2 caused a reduction in the size of the tumors within 5 days. The LLC-IL2 cells were then inoculated into the left flank of mice at 5-day intervals. Mice were inspected twice weekly and tumor volumes were calculated using the following formula: tumor volume = $LD^2/2$ (where L is the longest diameter and D the shortest diameter).

After the volume of each cytokine gene-transfected LLC tumor reached approximately 150 mm^3, TZT-1027 was administered i.v. to the mice twice at an interval of 7 days (q7d×2 schedule) at doses of 0.5, 1, 2 and 3 mg/kg. The dosing volume was 0.1 ml/10 g body weight. Control mice were treated with 0.05 *M* lactate buffer. Tumor growth inhibition (T/C) was calculated according to the formula: T/C(%) = [(tumor volume of treated mice) (tumor volume of control mice)] ×100. The experiments were completed within 1 month after inoculation of the mice, i.e. before the host's non-

Fig. 1 The chemical structure of TZT-1027

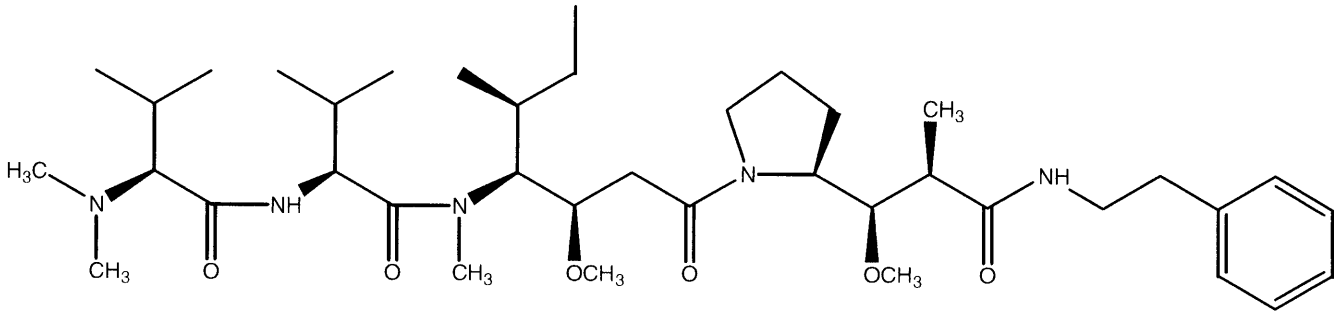

specific immune defenses began to manifest themselves. All experiments were performed twice.

Immunohistochemical analysis

Histological sections were taken from the LLC-Neo, LLC-TNF and LLC-IL6 tumor tissues from untreated control mice and at 72 h after i.v. administration of a single dose of 2 mg/kg TZT-1027. After removal, tumor tissues were immediately embedded and frozen in Tissue-Tek OCT compound (Miles Laboratories, Elkhart, Tenn.), and sections were cut at 8 μm thickness. Tissue sections were dried and immersed in acetone at –20°C and endogenous peroxidase activity was quenched with 0.03% hydrogen peroxidase in phosphate-buffered saline (PBS) for 10 min at room temperature. They were washed in PBS and blocked with 5% goat serum for 30 min at room temperature. The tissue sections were then incubated with primary antibody (rat anti-mouse CD31 antibody) diluted 1:500 overnight at 4°C. They were washed several times in PBS, and incubated with secondary antibody (goat biotinylated anti-rat IgG antibody: Vector Laboratories, Burlingame, Calif.) diluted 1:300 for 30 min at room temperature. After several washes in PBS, the antibody was visualized using a Vectastain ABC Elite kit. Peroxidase binding was demonstrated by the addition of diaminobenzidine. Subsequently, counterstaining using hematoxylin was performed to investigate nuclear location.

RNA isolation

Total RNA was obtained from LLC-Neo, LLC-TNF and LLC-IL6 tumor tissues by a single-step guanidinium thiocyanate procedure with or without administration of a single dose of 2 mg/kg TZT-1027 24 h earlier. PolyA$^+$ RNA was prepared with a poly(A) Quick mRNA isolation kit (Stratagene, La Jolla, Calif.) following the manufacturer's protocol.

cDNA expression macroarray

Differences in gene expression among LLC-Neo, LLC-TNF and LLC-IL6 tumor tissues in the flanks of mice untreated or treated i.v. with TZT-1027 were assessed with an Atlas Mouse cDNA array (Clontech, Palo Alto, Calif.). Each polyA$^+$ RNA (1 μg) was converted into ^{32}P-labelled first-strand cDNA with MMLV reverse transcriptase, and unincorporated ^{32}P-labelled nucleotides were removed by Chroma Spin-200 column chromatography. cDNA fractions with the highest activity were pooled and hybridized to one of the Atlas membranes on which 588 different gene fragments had already been crosslinked. The heat-denatured probe was added about 30 min after prehybridization with Express Hyb (Clontech) at 70°C and supplemented with 150 μg/ml of sonicated salmon sperm DNA (Stratagene), and hybridization was performed overnight at 68°C. Membranes were washed in 2× SSC/1% SDS at 70°C four times, followed by washing in 0.1× SSC/0.5% SDS at 70°C twice. After washing, the membranes were sealed in a Gel Bond film (FMC Bio Products, Rockland, Me.), and exposed to an imaging plate (BAS-III2040; Fuji Film Company, Tokyo, Japan) for 1 to 3 days. The images were analyzed densitometrically by scanning with a BAS-2000II (Fuji Film Company), and the density of each spot was quantified with an Array Gauge (version 1; Fuji Film Company). Gene expression in the samples was adjusted for the total density level of each membrane, instead of comparing it with the expression of the human housekeeping genes included in the membranes.

Statistical analysis

The significances of differences between TZT-1027-treated and vehicle-treated mice inoculated with cytokine gene-transfected LLCs and between TZT-1027-treated mice inoculated with cytokine gene-transfected LLCs and TZT-1027-treated mice inoculated with LLC-Neo were evaluated using Student's or Welch's *t*-tests.

Results

The in vitro growth-inhibitory effects of TZT-1027 against various cytokine gene-transfected LLCs cells determined by MTT assay

TZT-1027 exposure for 72 h inhibited the growth of various cytokine gene-transfected LLC cells (i.e. LLC,

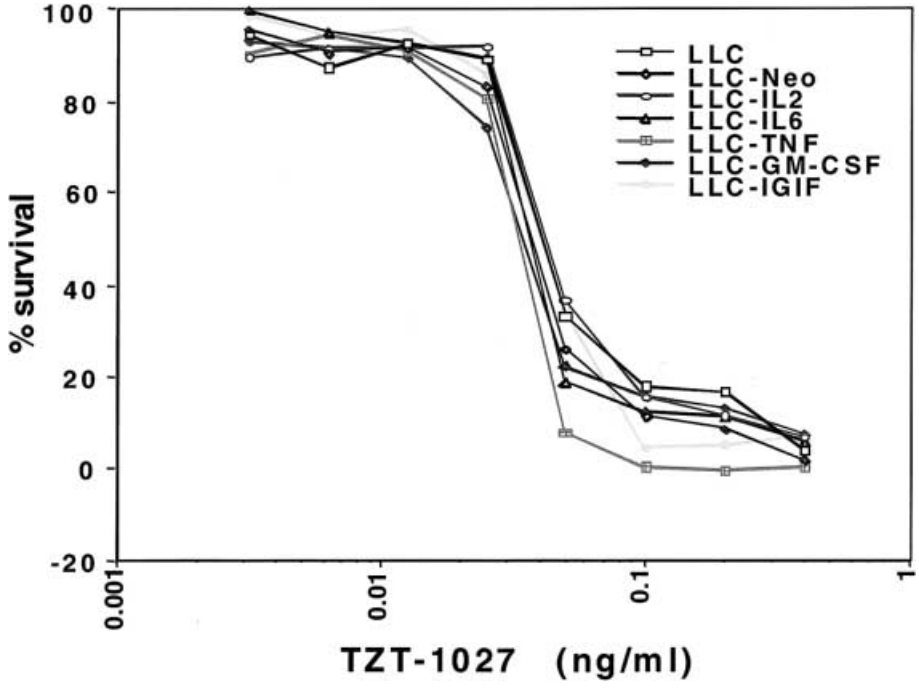

Fig. 2 The growth inhibitory effects of TZT-1027 against various cytokine gene-transfected LLCs in vitro determined by the MTT assay

LLC-Neo, LLC-IL2, LLC-IL6, LLC-TNF, LLC-GM-CSF and LLC-IGIF) with an IC_{50} range of 0.03 to 0.05 ng/ml, as determined by the MTT assay (Fig. 2). No marked difference in growth-inhibitory effects on these cell lines was observed in vitro.

Antitumor effect of TZT-1027 on various cytokine gene-transfected LLC tumors in C57BL/6 mice

To elucidate the interactions between cytokines and TZT-1027 in vivo, we examined the antitumor activities of TZT-1027 in a variety of cytokine gene-transfected LLC tumors in C57BL/6 mice. On a q7d×2 schedule, i.v. administration of TZT-1027 produced dose-dependent inhibition of tumor growth against LLC tumors: 2 mg/kg TZT-1027 produced an approximately 50% reduction in tumor volume as compared with vehicle treatment, while 3 mg/kg TZT-1027 produced an 80% inhibition. These results are presented in Fig. 3. TZT-1027 also exerted similar inhibitory effects against LLC-Neo tumors (data not shown). Thus, the effective doses were considered to be 2 and 3 mg/kg.

The rates growth of each cytokine gene-transfected LLC tumor were approximately the same except for the slightly slower growth of LLC-TNF tumor, possibly owing to the effect of TNF-α. TZT-1027 was administered i.v. to C57BL/6 bearing various cytokine gene-transfected LLC tumors at a dose of 2 or 3 mg/kg on a q7d×2 schedule. The results are shown in Table 1. T/C values for 2 and 3 mg/kg TZT-1027 were 36% and 16%, respectively, against LLC-Neo tumors. TZT-1027 was more effective against LLC-TNF tumors with T/C values of 10% and 4% for 2 and 3 mg/kg, respectively. TZT-1027 was also effective against LLC-IL6 tumors with T/C values of 11% and 3% for 2 and 3 mg/kg, respectively. The significance of the differences was determined using Student's or Welch's *t*-tests in all of the TZT-1027-treated mice bearing cytokine gene-transfected LLC tumors compared with vehicle-treated control mice. The significance of the differences in T/C values was also determined using Welch's *t* test in TZT-1027-treated mice bearing LLC-TNF or LLC-IL6 tumors in comparison with TZT-1027-treated mice bearing LLC-Neo tumors. The results suggest that TZT-1027 had stronger in vivo antitumor effect on the tumors secreting TNF-α and IL-6.

Immunohistochemical analysis

Enhanced antitumor effects were observed in TZT-1027-treated mice bearing LLC-TNF and LLC-IL6 tumors. We focused on the effect on the tumor vasculature which might be the cause of the enhanced antitumor activity. Therefore, we stained the vessels of the transplanted cytokine gene-transfected LLC tumors with anti-CD31 antibody immunohistochemically. The vasculature of LLC-TNF and LLC-IL6 tumors showed stronger staining with anti-CD31 antibody than did LLC-Neo tumors, suggesting that LLC-TNF and LLC-IL6 tumors had a highly vascular structure (Fig. 4a, c and e). In TZT-1027-treated mice, LLC-Neo, LLC-TNF and LLC-IL6 tumors were diffusely rather than focally stained (Fig. 4b, d and f), indicating destruction of tumor vessels. The destruction was more marked in LLC-TNF and LLC-IL6 tumors. These results suggest that TZT-1027 destroys tumor vasculature as well as the tumor itself in a process that involves TNF-α or IL-6.

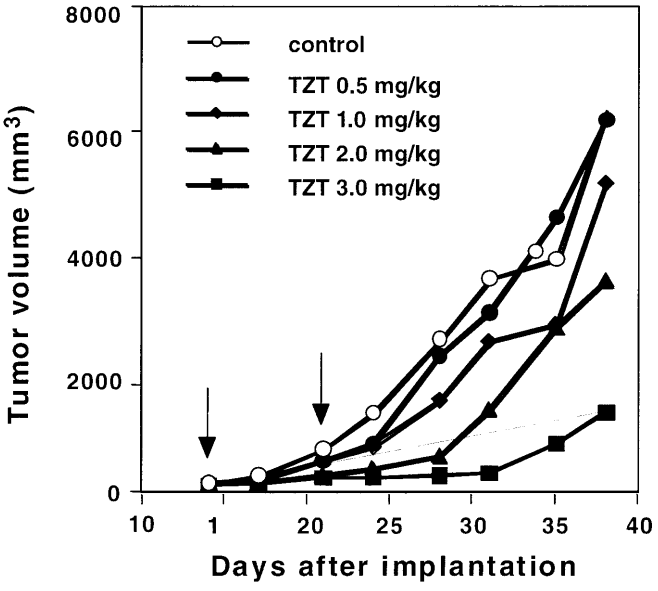

Fig. 3 The inhibitory effect of TZT-1027 against the growth of LLC tumors inoculated into C57BL/6 mice. *Arrows* show the days of TZT-1027 administration

Table 1 Antitumor activity of TZT-1027 administered twice at an interval of 7 days (q7d×2 schedule) against various cytokine gene-transfected LLC tumors in terms of T/C (tumor size of treated mice/tumor size of control mice ×100) determined 14 days after the final TZT-1027 administration

Tumor	T/C (%)	
	TZT-1027 (2 mg/kg)	TZT-1027 (3 mg/kg)
LLC	23*	11*
LLC-Neo	36*	16*
LLC-TNF	10*,**	4*,**
LLC (LLC-IL2)	20*	22*
LLC-IL6	11*,**	3*,**
LLC-IGIF	35*	38*

*$P < 0.05$ vs control, Student's or Welch's *t*-test; **$P < 0.05$ vs LLC-Neo at the same dose, Welch's *t*-test

Gene expression profile of cytokine transfectant tumors in mice treated with TZT-1027

To investigate the molecular mechanisms involved in the enhancement of in vivo TZT-1027 antitumor activity in

mice bearing LLC-TNF and LLC-IL6 tumors, we examined the expression of hundreds of tightly transcriptionally controlled genes in the tumors. In order to assess the relatively early time period after administration of TZT-1027, the tumors were removed 24 h after the administration of TZT-1027, and the mRNA was purified and examined using the cDNA macroarray. The differential gene expression patterns of LLC-Neo, LLC-TNF and LLC-IL6 tumor tissues from mice untreated or treated with TZT-1027 were examined using a cDNA macroarray (Fig. 5), and the majority of the altered mRNA was selected densitometrically followed by the use of Array Gauge analytical software. For standardization, all the density data were obtained by subtracting the minimum density among all the spots. The mem-

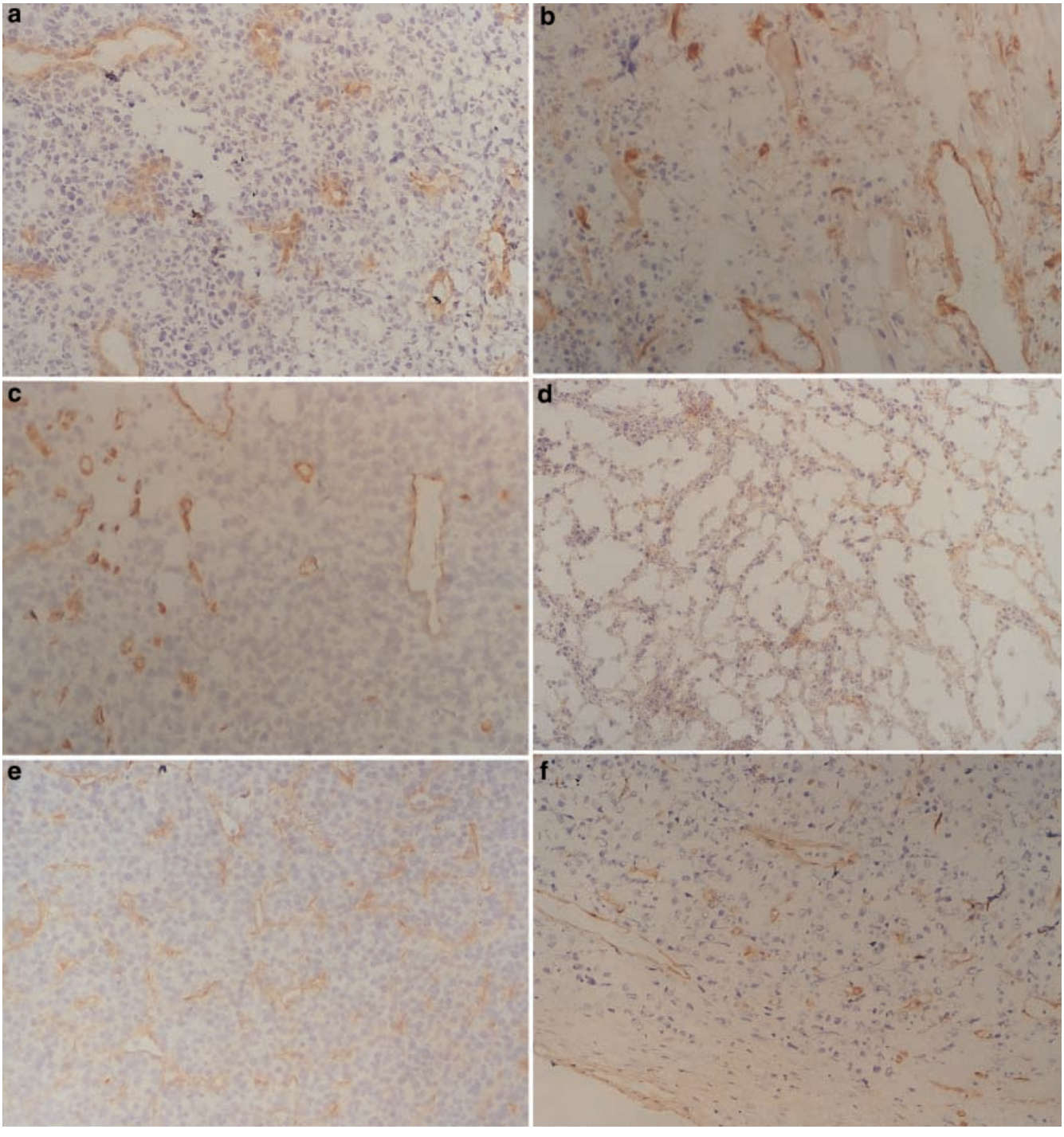

Fig. 4a–f Immunohistochemical analysis of LLC tumor tissues in mice treated or untreated with TZT-1027 using anti-CD31 antibody which stains vascular endothelial cells. **a**, **b** LLC-Neo tissue in untreated and TZT-1027-treated mice; **c**, **d** LLC-TNF tissue in untreated and TZT-1027-treated mice; **e**, **f** LLC-IL6 tissue in untreated and TZT-1027-treated mice

branes were standardized using the median values of all the spots in each membrane. The ratios of each gene spot for the LLC-Neo, LLC-TNF and LLC-IL6 tissue samples, from mice both untreated and treated with TZT-1027, were calculated. The factors involved in the combined effects of TNF-α or IL-6 and TZT-1027 are shown in Tables 2 and 3. We compared the expression profile of LLC-Neo tumors from mice treated with TZT-1027 with the expression profiles of LLC-TNF and LLC-IL6 tumors.

Additional alterations in gene expression were observed in LLC-TNF tumors in response to TZT-1027 treatment, as compared with LLC-Neo tumors in mice treated with TZT-1027 and LLC-TNF tumors (Table 4). Similarly, further alterations in gene expression were observed in LLC-IL6 tumors as compared with LLC-Neo tumors in mice treated with TZT-1027 and LLC-IL6 tumors (Table 5). The commonly altered factors associated with the enhanced antitumor activity seen in LLC-TNF and LLC-IL6 tumors from mice treated with TZT-1027 were then revealed to be the non-histone chromosomal protein HMG-14 and the transcription factor 1 for heat shock gene. Although PKC-theta gene was highly expressed in LLC-TNF tumors from mice treated with TZT-1027 (Table 4), this gene was not altered in LLC-IL6 tumors from mice treated with TZT-1027 (the expression ratio was 1.16). We assumed that genes altered more than threefold were significantly altered genes. On this basis, therefore, PKC-theta was not selected as a commonly altered factor.

The enhanced antitumor activity of TZT-1027 in LLC-TNF and LLC-IL6 tumors was conceivably due to the destruction of the tumor vasculature. We therefore focused on the alteration of mRNAs related to angiogenesis, and the results are shown in Table 6. Alterations in mRNAs including ICAM1, VCAM1, selectin, integrins, PAI-2, TNF-α, TPA, UPA, TIMP-3, iNOS, MIP-1α receptor, laminin receptor and TNFR1 were observed. Marked modulation of transcription factors such as ets family genes and homeobox family genes was also observed. These factors may be responsible for the enhanced antitumor activity of TZT-1027 in association with the cytokines studied.

Fig. 5a–c The alteration in mRNAs in LLC-TNF and LLC-IL6 tissues in mice treated with TZT-1027 (**a** LLC-Neo tissue, **b** LLC-TNF tissue, **c** LLC-IL6 tissue)

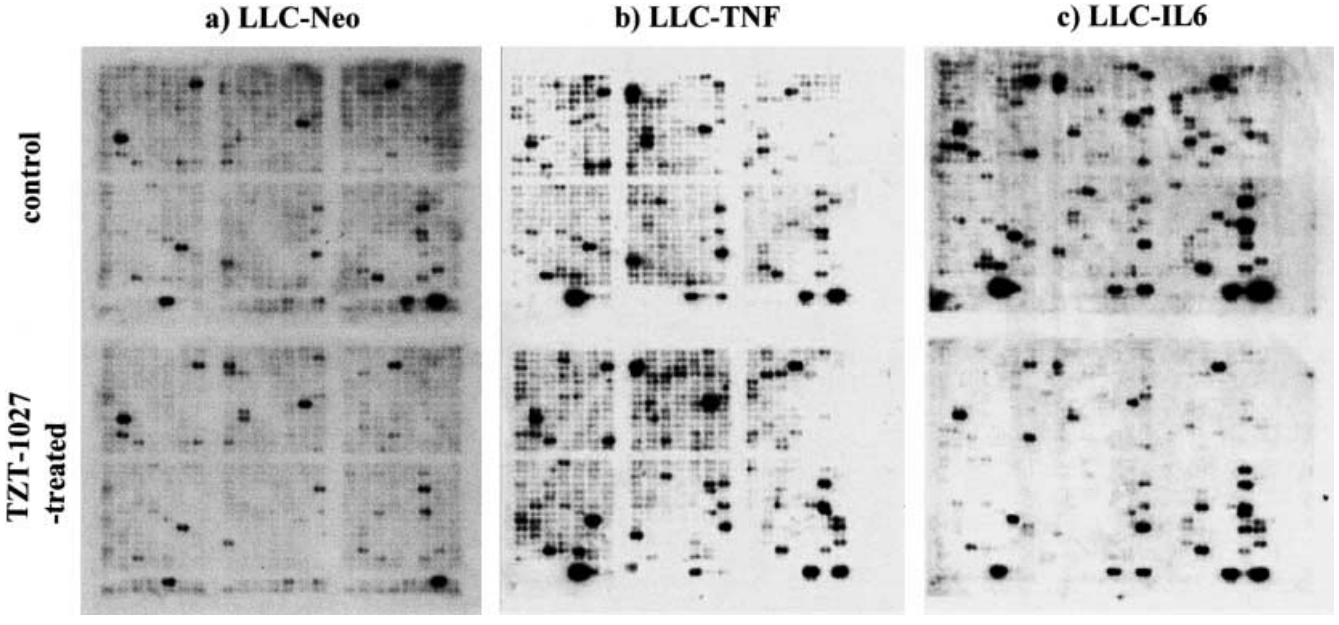

Discussion

As shown in Fig. 2, the growth-inhibitory effects of TZT-1027 on various cytokine gene-transfected LLC cells did not differ among the cell lines in vitro. Therefore, the enhanced antitumor effects of TZT-1027 in mice bearing LLC-TNF and LLC-IL6 tumors to be attributable to certain in vivo factors (Table 1).

Some hypotheses were raised to explain these effects. TNF-α and IL-6 alone can induce antitumor effects. TNF-α is induced by the activation of host macrophages which leads to its antitumor effects [6, 12, 22, 26, 35], and TNF-α and IL-6 have been reported to exert a damaging effect on tumor vasculature [13, 25, 28, 46]. Furthermore, the synergistic effects of TNF-α and IL-6 with antimicrotubule agents in vitro have also been investigated, although the results obtained are somewhat inconsistent [1, 4, 48, 53]. In particular, synergistic effects with such antimicrotubule agents as vinblastine have not yet been shown in vitro. In contrast, this study demonstrated enhanced antitumor activity of the antimicrotubule agent, TZT-1027, in tumors secreting TNF-α or IL-6.

Almost the same results have been observed by other groups. Recently, Mohammad et al. have reported that a

Table 2 Common alterations in mRNAs in LLC-Neo tissue from mice treated with TZT-1027 and in LLC-TNF tissue compared with LLC-Neo tissue

Gene	Coordinate	Ratio[a]	Ratio[b]
Oncogenes and tumor suppressors			
c-re1 proto-oncogene	A-2-m	4.64	3.28
Ear-2; v-erbA-related proto-oncogene	A-2-n	6.40	5.59
Intercellular signal transduction modulators and effectors			
C-C chemokine receptor type 1 (C-C CKR-1, CCR-1); macrophage inflammatory protein-1 alpha receptor (MIP-1alpha-R); RANTES-R	B-2-i	3.67	6.21
Apoptosis protein			
Defender against cell death 1 (DAD1)	C-3-d	0.32	0.30
Transcription factors and general DNA-binding proteins			
Transcription factor COE1; early B-cell factor (EBF)	D-2-a	3.80	4.31
Engrailed homeobox protein (EN1; MOEN1)	D-2-b	3.09	3.51
Ets-related transcription factor; E74-like factor 1 (ELF1)	D-2-j	4.22	3.20
Erf; Ets-related transcription factor	D-2-m	3.94	3.80
Erythroid Kruppel-like transcription factor (EKLF)	D-2-n	4.74	3.65
Ets-related protein PEA 3	D-3-a	4.65	5.81
C-ets2	D-3-b	6.53	5.98
Ets-related protein Sap 1A	D-3-c	4.45	4.83
Homeobox protein 3.1(Hox-3.1)	D-4-d	3.06	10.56
Ikaros DNA-binding protein	D-4-i	3.66	19.44
Interferon inducible protein 1	D-4-k	3.82	8.37
Interferon regulatory factor 2 (IRF 2)	D-4-l	3.70	7.08
Lbx 1 transcription factor	D-4-n	3.48	5.94
SRY-box containing gene 3 (Sox3)	D-5-n	3.70	5.85
Growth factors and chemokines receptors			
Activin type I receptor	E-1-a	3.32	3.88
Neurotransmitter receptors			
Nicotinic acetylcholine receptor	E-5-k	3.15	6.90
Cell surface antigens and cell adhesion molecules			
40S ribosomal protein SA; p40-8; laminin receptor 1 (LAMR1); 34/67 kDa laminin receptor	E-7-j	0.12	3.87

[a]Alteration in mRNAs in LLC-Neo tissue of mice after TZT-1027 administration
[b]Alteration in mRNAs in LLC-TNF tissue compared with LLC-Neo tissue

compound identical to TZT-1027 shows antitumor activity superior to that of its mother compound, dolastatin 10, in SCID mice bearing human diffuse large-cell lymphoma cells (WSU-DLCL$_2$) and human B-cell chronic lymphocytic leukemia cells (WSU-CLL) [32, 33]. They also observed a synergistic effect of this compound in combination with bryostatin 1 in the same xenograft model [32, 33]. Another group has reported that bryostatin 1 enhances the expression of some cytokines including TNF-α and IL-6 in human peripheral blood monocytes and the possibility of bryostatin 1 inducing these cytokines in other immune cells was discussed [7]. Therefore, the synergistic effect of this compound in combination with bryostatin 1 could be due to enhanced production of TNF-α and IL-6 by bryostatin 1.

It is interesting that TZT-1027 was more potent against tumor cells in vitro (IC_{50} values in the nanomolar range) than in the tubulin polymerization assay (IC_{50} values in the micromole range). This prominent antitumor effect in vitro could indicate that TZT-1027 acts by another antitumor mechanism. We propose that TZT-1027 exerts a potent effect on the tumor vasculature. Previous studies have demonstrated that antimicrotubule agents, including dolastatin 10, vinblastine, vincristine and combretastatin A-4 induce vascular injury, enhance vascular permeability, promote thrombosis and decrease tumor blood flow [2, 9, 11, 18, 19, 39]. It has also been suggested that TZT-1027 can exert these effects on tumor vasculature [44].

To determine which molecules are involved in the enhanced antitumor effects observed in LLC-Neo-, LLC-TNF- and LLC-IL6-bearing C57BL/6 mice, we identified the altered genes in mice both untreated and treated with TZT-1027, using a cDNA macroarray. We have previously demonstrated gene expression profiles in cultured cells exposed to TZT-1027 in vitro [37]. We examined gene expression in tumor tissues from inoculated mice, as this is closer to the clinical situation.

Although the enhanced antitumor effects of TZT-1027 in LLC-TNF and LLC-IL6 tumors could have been a result of the exogenous effects of the cytokines, we believe that these variations could have been a result of the genetic alterations in the tumor cells. To support this idea, we are planning to investigate the effects of a combination of TZT-1027 and exogenously administered cytokines on the growth of the parental cell line. We focused on altered genes involved in the effects of TZT-1027 (LLC-Neo tumors in mice untreated and

Table 3 Common alterations in mRNAs in LLC-Neo tissue from mice treated with TZT-1027 and in LLC-IL6 tissue compared with LLC-Neo tissue

Gene	Coordinate	Ratio[a]	Ratio[c]
Oncogenes and tumor suppressors			
C-myc proto-oncogene	A-2-l	3.21	4.80
C-re1 proto-oncogene	A-2-m	4.64	8.41
Ear-2; v-erbA related proto-oncogene	A-2-n	6.40	12.24
Cell cycle regulators			
G1/S-specific cyclin Dl (CCND1; CYL-1)	A-6-f	0.32	3.21
Stress response proteins			
84-kDa heat shock protein (HSP84); HSP 90-beta; tumor-specific transplantation 84-kDa antigen (TSTA, HSPCB)	B-1-c	3.28	5.38
Transcription factors and general DNA-binding protein			
Transcription factor COE1; early B-cell factor (EBF)	D-2-a	3.80	6.55
Engrailed homeobox protein (EN1; MOEN1)	D-2-b	3.09	5.26
Ets-related transcription factor; E74-like factor 1 (ELF1)	D-2-j	4.22	3.38
Erf; Ets-related transcription factor	D-2-m	3.94	4.70
Erythroid Kruppel-like transcription factor (EKLF)	D-2-n	4.74	5.15
Ets-related protein PEA 3	D-3-a	4.65	7.75
C-ets2	D-3-b	6.53	6.99
Ets-related protein Sap 1A	D-3-c	4.45	5.42
Homeobox protein 3.1 (Hox-3.1)	D-4-d	3.06	9.86
Ikaros DNA binding protein	D-4-i	3.66	15.45
Interferon inducible protein 1	D-4-k	3.82	14.57
Interferon regulatory factor 2 (IRF 2)	D-4-l	3.70	35.79
Lbx 1 transcription factor	D-4-n	3.48	8.73
SRY box-containing gene 3 (Sox3)	D-5-n	3.70	11.63

[a]Alteration in mRNAs in LLC-Neo tissue of mice after TZT-1027 administration
[c]Alteration in mRNAs in LLC-IL6 tissue of mice compared with LLC-Neo tissue

Table 4 Alteration in mRNAs in LLC-TNF tissue from mice treated with TZT-1027

Gene	Coordinate	Ratio
Oncogenes and tumor suppressors		
Transcription termination factor 1 (TTF1)	A-2-j	10.37
Intercellular signal transduction modulators and effectors		
I-kappa B alpha subunit (IKB alpha)	B-3-m	3.35
PKC-theta	B-6-h	73.57
Apoptosis protein		
Tumor necrosis factor receptor 1 precursor (TNFR1); TNFRSF1A	C-5-b	0.33
Transcription factors and general DNA-binding proteins		
Butyrate response factor 1	D-1-i	3.06
Non-histone chromosomal protein HMG-14	D-3-m	4.52
Split hand/foot gene	D-5-m	9.38
Transcription factor 1 for heat shock gene	D-6-i	132.72
cAMP-dependent transcription factor 3 (ATF3); activating factor 3; transcription factor LRG-21	D-6-n	3.11
Protein turnover (proteases and inhibitors)		
Serine protease inhibitor 2-2 (SPI2-2); SPI2 proteinase inhibitor; SPI2/EB4	F-7-j	3.13

treated with TZT-1027), TNF-α (LLC-TNF tumors compared with LLC-Neo tumors) and IL-6 (LLC-IL6 tumors compared with LLC-Neo tumors). We also selected genes to which the enhanced antitumor activity observed in mice bearing LLC-TNF or LLC-IL6 tumors and treated with TZT-1027 could be attributed. Notably, among these genes we focused on those newly and independently altered by the combined effect of TZT-1027 and TNF-α, or of TZT-1027 and IL-6. The commonly altered genes in these two tissues were revealed to be the non-histone chromosomal protein HMG-14 and the transcription factor 1 for heat shock gene. Additionally, we focused on alterations in the expression of genes related to angiogenesis. Modulation of transcriptional factors such as ets family genes and homeobox family genes was found. These genes could be important determinants of enhanced antitumor activity.

HMG-14 is a chromosomal protein. It enhances the transcriptional potential of chromatin when incorporated into nucleosomes during, but not after, chromatin

Table 5 Alteration in mRNAs in LLC-IL6 tissue from mice treated with TZT-1027

Gene	Coordinate	Ratio
Oncogenes and tumor suppressors		
C-myb proto-oncogene protein	A-2-k	3.75
JunD	A-3-g	3.70
Cell cycle regulators		
Tob antiproliferative factor; interacts with p 185erbB2	A-7-n	3.34
Apoptosis protein		
Plasma glutathione peroxidase precursor (GSHPX-P): GPX3	C-1-l	3.11
NADPH-cytochrome P450 reductase (CPR); POR	C-4-a	0.33
Programmed cell death 1 protein precursor (PDCD-1; PD-1)	C-4-f	0.33
T-cell death-associated protein (TDAG51)	C-5-a	0.32
Transcription factors and general DNA-binding protein		
Epidermal growth factor receptor kinase substrate EPS8	D-2-k	3.10
Non-histone chromosomal protein HMG-14	D-3-m	3.12
Transcription factor 1 for heal shock gene	D-6-i	3.21
Growth factors and chemokines receptors		
D-factor/LIF receptor	E-1-l	0.19
ERBB-2 receptor: c-neu: HER2 protein tyrosine kinase	E-1-m	0.31
Interleukin and interferon receptors		
Interleukin-9 receptor (IL9R)	E-3-i	0.23
Hormone receptors		
Prolactin receptor PALR2	E-4-c	0.21
Neurotransmitter receptors		
5-Hydroxytryptamine (serotonin) receptor 1c	E-4-g	0.31
Cell surface antigens and cell adhesion molecules		
P-selectin glycoprotein ligand 1 precursor (PSGL1; SELPLG: SELP1)	E-5-I	3.68
CD14 monocyte differentiation antigen precursor: LPS receptor (LPSR): myeloid cell-specific leucine-rich glycoprotein	E-6-h	5.42
CD22 antigen	E-6-i	3.25
Fibronectin receptor beta subunit precursor: integrin beta 1 (ITGB1)	E-7-g	4.86
Integrin beta 7	E-7-h	3.56
Neural cadherin precursor (N-cadherin: CDH2)	E-7-k	5.19
Growth factors, cytokines and chemokines		
Insulin-like growth factor binding protein -6(IGFBP 6)	F-2-i	3.60
Macrophage inflammatory protein 2 alpha (M1P2-alpha)	F-3-g	12.98
Glucose-6-phosphate isomerase (GPI) phosphoglucose isomerase (PGI) phosphohexose isomerase (PHI); neuroleukin (NLK)	F-3-m	3.70
Thromboprotein precursor (THPO); megakaryocyte colony-stimulating factor (MCSF): c-mpl ligand (ML): megakaryocyte growth and development factor (MGDF)	F-4-e	0.30
Transforming growth factor beta 2 precursor (TGF-beta 2: TGFB2)	F-4-g	0.27
Tumor necrosis factor beta (TNF-beta): lymphotoxin-alpha	F-4-h	0.19
Cytoskeleton and motility proteins		
Cardiac myosin heavy subunit alpha isoform (MYH6: MYHCA)	F-5-e	0.32
Type II cytoskeletal keratin1 (KRT2-1): cytokeratin 1 (KRT1); 67-kDa cytokeratin	F-5-k	0.18
Kinesin family protein KIF 1A	F-5-m	0.19
Non-muscle myosin light chain 3 (MLC3NM: MYLN): MYL6	F-6-b	8.45
Vimentin (VIM)	F-6-d	4.06
Protein turnover (proteases and inhibitors)		
Cathepsin B1 (CTSB)	F-6-g	5.29
Cathepsin D (CTSD)	F-6-h	6.36
Cathepsin H	F-6-i	3.31
Tissue plasminogen activator precursor (T-plasminogen activator: PLAT: TPA)	F-7-e	0.23
Urokinase type plasminogen activator	F-7-f	0.15
Tissue inhibitor of metalloproteinases 3 (TIMP3); SUN	F-7-n	0.25

assembly on replicating DNA. Although the interaction between HMG-14 and microtubule or antimicrotubule agents is unknown, HMG-14 has been reported to bind MAP kinase [3]. Therefore, some interaction between HMG-14 and microtubules is plausible. On the other hand, the transcription factor 1 for heat shock gene is the key transcriptional regulator of heat shock genes that protects cells from environmental stress. Similarly, although the interaction between transcription factor 1 for heat shock gene and microtubule or antimicrotubule agents is unknown, the upregulation of this factor appears to be a protective response of these tissues to the

Table 6 Alterations in mRNAs related to angiogenesis

Gene	Coordinate	Ratio
mRNAs in LLC-Neo tissue of mice after TZT-1027 administration		
C-C chemokine receptor type 1 (C-C CKR-1; CCR-1); macrophage inflammatory protein-1 alpha receptor (MIP-alpha-R); RANTES-R	B-2-i	3.67
LFA1-alpha: integrin alpha L; leukocyte adhesion glycoprotein LFA-1 alpha chain; antigen CD11A (p180)	B3-e	0.32
Inducible nitric oxide synthase (INOS); type II NOS macrophage NOS; NOS2	C-3-m	3.46
Ets-related transcription factor: E74-like factor 1 (ELF1)	D-2j	4.22
Erf; Ets-related transcription factor	D-2-m	3.94
Ets-related protein PEA 3	D-3-a	4.65
c-ets2	D-3-b	6.53
Ets-related protein Sap 1A	D-3-c	4.45
Homeobox protein 3.1(Hox-3.1)	D-4-d	3.06
Cell surface glycoprotein MAC-1 alpha subunit precursor; CR-3 alpha subunit; CD11B antigen; leukocyte adhesion receptor MO1; integrin alpha-M (ITGAM)	E-6-j	0.20
Intercellular adhesion molecule 1 precursor (ICAM1); MALA2	E-7-i	0.18
40S ribosomal protein SA p40-8; laminin receptor 1 (LAMR1); 34/67-kDa laminin receptor	E-7-j	0.12
vascular cell adhesion protein 1	E-7-m	0.19
mRNAs in LLC-TNF tissue compared with LLC-Neo tissue		
C-C chemokine receptor type 1 (C-C CKR-1; CCR-1); macrophage inflammatory protein-1 alpha receptor (MIP-1alpha-R); RANTES-R	B-2-i	6.21
Erf; Ets-related transcription factor	D-2-m	3.80
Ets-related protein PEA 3	D-3-a	5.81
C-ets2	D-3-b	5.98
Ets-related protein Sap 1A	D-3-c	4.83
Homeobox protein 1.1 (Hox-1.1)	D-3-n	4.04
Homeobox protein 2.4 (Hox-2.4)	D-4-b	4.46
Homeobox protein 2.5 (Hox-2.5)	D-4-c	6.64
Homeobox protein 3.1 (Hox-3.1)	D-4-d	10.56
Homeobox protein D4 (HOXD4); HOX-4.2; HOX-5.1	D-4-e	3.93
Homeobox protein 7.1 (Hox-7.1)	D-4-f	3.50
Homeobox protein HOXD-3	D-4-h	5.52
P-selectin glycoprotein ligand 1 precursor (PSGL1; SELPLG; SELP1)	E-5-l	3.47
mRNAs in LLC-IL6 tissue compared with LLC-Neo tissue		
Ets-domain protein elk3; ets-related protein net; ERP	A-3-i	6.78
Ets-related transcription factor; E74-like factor 1 (ELF1)	D-2-j	3.38
Erf; Ets-related transcription factor	D-2-m	4.70
Ets-related protein PEA 3	D-3-a	7.75
C-ets2	D-3-b	6.99
Ets-related protein Sap 1A	D-3-c	5.42
Homeobox protein 1.1 (Hox-1.1)	D-3-n	4.20
Homeobox protein B5 (HOXB5); HOX-2.1; MU; H24.1	D-4-a	3.00
Homeobox protein 2.4 (Hox-2.4)	D-4-b	4.66
Homeobox protein 2.5 (Hox-2.5)	D-4-c	6.31
Homeobox protein 3.1 (Hox-3.1)	D-4-d	9.86
Homeobox protein D4 (HOXD4); HOX-4.2; HOX-5.1	D-4-e	3.58
Homeobox protein 7.1 (Hox-7.1)	D-4-f	3.23
Homeobox protein HOXD-3	D-4-h	4.49
Fibroblast growth factor 9	F-1-k	0.21
Macrophage plasminogen activator inhibitor 2 (PAI2; PLANH2)	F-7-i	0.33
mRNAs in LLC-TNF tissue after TZT-1027 administration		
Tumor necrosis factor receptor 1 precursor (TNFR1); TNFRSF1A	C-5-b	0.33
Ets-related transcription factor; E74-like factor 1 (ELF1)	D-2-j	3.90
Erf; Ets-related transcription factor	D-2-m	3.79
Ets-related protein PEA 3	D-3-a	5.40
C-ets2	D-3-b	6.30
Ets-related protein Sap 1A	D-3-c	4.76
Homeobox protein 1.1 (Hox-1.1)	D-3-n	4.05
Homeobox protein 2.4 (Hox-2.4)	D-4-b	4.48
Homeobox protein 2.5 (Hox-2.5)	D-4-c	6.59
Homeobox protein 3.1 (Hox-3.1)	D-4-d	10.48
Homeobox protein D4 (HOXD4); HOX-4.2; HOX-5.1	D-4-e	3.93
Homeobox protein 7.1 (Hox-7.1)	D-4-f	3.55
Homeobox protein HOXD-3	D-4-h	5.37
P-selectin glycoprotein ligand 1 precursor (PSGL1; SELPLG; SELPl)	E-5-i	3.49

Table 6. (Contd.)

Gene	Coordinate	Ratio
mRNAs in LLC-IL6 tissue of mice after TZT-1027 administration		
Ets-domain protein elk3; ets-related protein net; ERP	A-3-i	4.88
Ets-related transcription factor: E74-like factor 1 (ELF1)	D-2-j	4.58
Erf; Ets-related transcription factor	D-2-m	4.92
Ets-related protein PEA 3	D-3-a	11.70
C-ets2	D-3-b	8.40
EIS-related protein Sap 1A	D-3-c	5.29
Homeobox protein 1.1 (Hox-1.1)	D-3-n	4.61
Homeobox protein 2.4 (Hox-2.4)	D-4-b	4.74
Homeobox protein 2.5 (Hox-2.5)	D-4-c	5.47
Homeobox protein 3.1 (Hox-3.1)	D-4-d	9.69
Homeobox protein D4 (HOXD4); HOX-4.2; HOX-5.1	D-4-e	3.03
Homeobox protein HOXD-3	D-4-h	3.30
P-selectin glycoprotein ligand 1 precursor (PSGL1; SELPLG; SELP1)	E-5-l	3.68
Cell surface glycoprotein MAC-1 alpha subunit precursor; CR-3 alpha subunit; CD11 B antigen; leukocyte adhesion receptor MO1; integrin alpha-M (ITGAM)	E-6-j	5.03
Fibronectin receptor beta subunit precursor; integrin beta 1 (ITGB1)	E-7-g	4.86
Integrin beta 7	E-7-h	3.56
Intercellular adhesion molecule 1 precursor (ICAM1); MALA2	E-7-i	4.89
40S ribosomal protein SA; p40-B; laminin receptor 1 (LAMR1); 34/67-kDa laminin receptor	E-7-j	5.89
Tumor necrosis factor beta (TNF-beta): lymphotoxin-alpha	F-4-h	0.19
Tissue plasminogen activator precursor (T-plasminogen activator; PLAT; TPA)	F-7-e	0.23
Urokinase type plasminogen activator	F-7-f	0.15
Macrophage plasminogen activator inhibitor 2 (PAI2; PLANH2)	F-7-i	6.04
Tissue inhibitor of metalloproteinases 3 (TIMP3); SUN	F-7-n	0.25

stress induced by TZT-1027. This factor has also been reported to bind MAP kinase [10], so that some interaction between the transcription factor 1 for heat shock gene and microtubules is plausible. Furthermore, microtubules themselves have been reported to bind to HSP70 at the microtubule organizing center [27].

The ets gene family encodes transcription factors for mesodermal cell development during the embryonal period [24, 50], and ets-1 plays an especially important role in angiogenesis, regulating the expression of proteases and the migration of endothelial cells [20]. Ets-1 protein interacts with the UPA gene enhancer and with the promoters of metalloproteinase genes [38, 51]. Several members of the homeobox gene family are expressed in endothelial cells, suggesting a role for these morphoregulatory mediators during angiogenesis. Stimulation of endothelial cells by bFGF, VEGF or TPA reportedly leads to the modulation of several homeobox genes including Hox D3, in some cases with the concomitant upregulation of integrin $\alpha v\beta 3$ and UPA [5, 8]. The reason for this gene family being upregulated in this study is unknown. However, the regulation of these transcriptional factors was apparently a potent effect. The interaction between gene modulation and upregulation requires further study.

In conclusion, TZT-1027 showed enhanced antitumor effects against LLC-TNF and LLC-IL-6 tumors, with the tumor vasculature being destroyed, and some candidates possibly responsible for the enhanced antitumor effects were identified using a cDNA macroarray, although it will be necessary to analyze their expression at the transcriptional level and their products by conventional techniques such as Northern and Western blotting.

Acknowledgements This work was supported in part by Grants-in-Aid for Cancer Research from the Second Term of the Comprehensive Ten-Year Strategy for Cancer Control, the Ministry of Health and Welfare, and the Ministry of Education, Science and Culture of Japan.

References

1. Aoyama M, Maclsaac D, Bukowski RM, Ganapathi MK (1998) Interleukin 6 differentially potentiates the antitumor effects of Taxol and vinblastine in U266 human myeloma. Clin Cancer Res 4:1039
2. Baguley BC, Holdaway KM, Thomsen LL, Zhuang L, Zwi LJ (1991) Inhibition of the growth of colon 38 adenocarcinoma by vinblastine and colchicine: evidence for a vascular mechanism. Eur J Cancer 27:482
3. Barratt MJ, Hazzalin CA, Zhelev N, Mahadevan LC (1994) A mitogen- and anisomycin-stimulated kinase phosphorylates HMG-14 in its basic amino-terminal domain in vivo and isolated mononucleosomes. EMBO J 13:4524
4. Baumgart J, Schlott B, Suehnel J, Vater W, Schulze W, Behnke D (1991) Synergistic cytotoxicity of human recombinant tumor necrosis factor α combined with microtubule effectors. J Cancer Res Clin Oncol 117:239
5. Belotti D, Clausse N, Flagiallo D, Alami Y, Daukandt M, Deroanne C, Malfoy B, Boncinelli E, Faiella A, Castronovo V (1998) Expression and modulation of homeobox genes from cluster B in endothelial cells. Lab Invest 78:1291
6. Bogdan C, Ding A (1992) Taxol, a microtubule-stabilizing antineoplastic agent, induces expression of tumor necrosis factor alpha and interleukin-1 in macrophages. J Leukoc Biol 52:119
7. Bosco MC, Rottschafer S, Taylor LS, Ortaldo JR, Longo DL, Espinoza-Delgado I (1997) The antineoplastic agent bryostatin-1 induces proinflammatory cytokine production in human monocytes: synergy with interleukin-2 and modulation of interleukin-2Rγ chain expression. Blood 89:3402
8. Boudreau N, Andrews C, Srebrow A, Ravanpay A, Cheresh DA (1997) Induction of the angiogenic phenotype by Hox D3. J Cell Biol 139:257

9. Chaplin DJ, Pettit GR, Parkins CS, Hill SA (1996) Antivascular approaches to solid tumour therapy: evaluation of tubulin binding agents. Br J Cancer Suppl 27:S86
10. Chu B, Zhong R, Soncin F, Stevenson MA, Calderwood SK (1998) Transcriptional activity of heat shock factor 1 at 37 degrees C is repressed through phosphorylation on two distinct serine residues by glycogen synthase kinase 3 and protein kinases Calpha and Czeta. J Biol Chem 273:18640
11. Dark GG, Hill SA, Prise VE, Tozer GM, Pettit GR, Chaplin DJ (1997) Combretastatin A-4, an agent that displays potent and selective toxicity toward tumor vasculature. Cancer Res 57:1829
12. Ding A, Sanchez E, Nathan CF (1993) Taxol shares the ability of bacterial lipopolysaccharide to induce tyrosine phosphorylation of microtubule-associated protein kinase. J Immunol 151:5596
13. Fajardo FL, Kwan HH, Kowalski J, Prionas DS, Allison CA (1992) Dual role of tumor necrosis factor-α in angiogenesis. Am J Pathol 140:539
14. Felgner PL, Gadek TR, Holm M, Roman R, Chan HW, Wenz M, Northrop JP, Ringold GM, Danielsen M (1987) Lipofection: a highly efficient, lipid-mediated DNA-transfection procedure. Proc Natl Acad Sci U S A 84:7413
15. Ferrer FA, Miller LJ, Andrawis RI, Kurtzman SH, Albertsen PC, Laudone VP, Kreutzer DL (1998) Angiogenesis and prostate cancer: in vivo and in vitro expression of angiogenesis factors by prostate cancer cells. Urology 51:161
16. Fukumoto H, Nishio M, Nishio K, Heike Y, Arioka H, Kurokawa H, Ishida T, Fukuoka K, Nomoto T, Ohe Y, Saijo N (1997) Interferon-γ-inducing factor gene transfection into Lewis lung carcinoma cells reduces tumorigenicity in vivo. Jpn J Cancer Res 88:501
17. Heike Y, Takahashi M, Ohira T, Naruse I, Hama S, Ohe Y, Kasai T, Fukumoto H, Olsen KJ, Podack EE, Saijo N (1997) Genetic immunotherapy by intrapleural, intra peritoneal and subcutaneous injection of IL-2 gene-modified Lewis lung carcinoma cells. Int J Cancer 73:844
18. Hill SA, Lonergan SJ, Denekamp J, Chaplin DJ (1993) Vinca alkaloids: anti-vascular effects in a murine tumour. Eur J Cancer 29:1320
19. Hori K, Saito S, Nihei Y, Suzuki M, Sato Y (1999) Antitumor effects due to irreversible stoppage of tumor tissue blood flow: evaluation of a novel combretastatin A-4 derivative, AC7700. Jpn J Cancer Res 90:1026
20. Iwasaka C, Tanaka K, Abe M, Sato Y (1996) Ets-1 regulates angiogenesis by inducing the expression of urokinase-type plasminogen activator and matrix metalloproteinase-1 and the migration of vascular endothelial cells. J Cell Physiol 169:522
21. Karasuyama H, Melchers F (1988) Establishment of mouse cell lines which constitutively secrete large quantities of interleukin 2, 3, 4 or 5, using modified cDNA expression vectors. Eur J Immunol 18:97
22. Kirikae F, Kirikae T, Qureshi N, Takayama K, Morrison DC, Nakano M (1995) CD14 is not involved in *Rhodobacter sphaeroides* diphosphoryl lipid A inhibition of tumor necrosis factor alpha and nitric oxide induction by Taxol in murine macrophages. Infect Immun 63:486
23. Kobayashi M, Natsume T, Tamaoki S, Watanabe J, Asano H, Mikami T, Miyasaka K, Miyazaki K, Gondo M, Sakakibara K, Tsukagoshi S (1997) Antitumor activity of TZT-1027, a novel dolastatin 10 derivative. Jpn J Cancer Res 88:316
24. Kola I, Brooks S, Green AR, Grabber R, Tymms M, Papas T, Seth A (1993) The Ets1 transcription factor is widely expressed during murine embryo development and is associated with mesodermal cells involved in morphogenetic processes such as organ formation. Proc Natl Acad Sci USA 90:7588
25. Kuijpers TW, Raleigh M, Kavanagh T, Janssen H, Calafat J, Roos D, Harlan JM (1994) Cytokine-activated endothelial cells internalize E-selectin into a lysosomal compartment of vesiculotubular shape. A tubulin-driven process. J Immunol 152:5060
26. Lanni JS, Lowe SW, Licitra EJ, Liu JO, Jacks T (1997) p53-independent apoptosis induced by paclitaxel through an indirect mechanism. Proc Natl Acad Sci USA 94:9679
27. Marchesi VT, Ngo N (1993) In vitro assembly of multiprotein complexes containing α, β, and γ tubulin, heat shock protein HSP70, and elongation factor 1 α. Proc Natl Acad Sci USA 90:3028
28. Mawatari M, Kohno K, Mizoguchi H, Matsuda T, Asoh K, Damme JV, Welgus HG, Kuwano M (1989) Effect of tumor necrosis factor and epidermal growth factor on cell morphology, cell surface receptors, and the production of tissue inhibitors of metalloproteinases and IL-6 in human microvascular endothelial cells. J Immunol 143:1619
29. Merriman RL, Shackelford KA, Tanzer LR, Campbell JB, Bemis KG, Matsumoto K (1989) Drug treatments for metastasis of the Lewis lung carcinoma: lack of correlation between inhibition of lung metastasis and survival. Cancer Res 49:4509
30. Miles SA, Rezai AR, Salazar-Gonzales JF, Meyden MV, Stevens RH, Logan DM, Mitsuyasu RT, Taga T, Hirano T, Kishimoto T, Martinez-Maza O (1990) AIDS Kaposi sarcoma-derived cells produce and respond to interleukin-6. Proc Natl Acad Sci U S A 87:4068
31. Miyazaki K, Kobayashi M, Natsume T, Gondo M, Mikami T, Sakakibara K, Tsukagoshi S (1995) Synthesis and antitumor activity of novel dolastatin 10 analogs. Chem Pharm Bull 43:1706
32. Mohammad RM, Pettit GR, Almatchy VP, Wall N, Varterasian M, Al-Katib A (1998) Synergistic interaction of selected marine animal anticancer drugs against human diffuse large cell lymphoma. Anticancer Drugs 9:149
33. Mohammad RM, Varterasian ML, Almatchy VP, Hannoudi GN, Pettit GR, Al-Katib A (1998) Successful treatment of human chronic lymphocytic leukemia xenografts with combination biological agents auristatin PE and bryostatin 1. Clin Cancer Res 4:1337
34. Mosmann T (1983) Rapid colorimetric assay for cellular growth and survival: application to proliferation and cytotoxicity assays. J Immunol Methods 65:55
35. Mullins DW, Walker TM, Burger CJ, Elgert KD (1997) Taxol-mediated changes in fibrosarcoma-induced immune cell function: modulation of antitumor activities. Cancer Immunol Immunother 45:20
36. Natsume T, Watanabe J, Tamaoki S, Fujio N, Miyasaka K, Kobayashi M (2000) Characterization of the interaction of TZT-1027, a potent antitumor agent, with tubulin. Jpn J Cancer Res 91:737
37. Natsume T, Nakamura T, Koh Y, Kobayashi M, Saijo N, Nishio K (2002) Gene expression profiling of exposure to TZT-1027, a novel microtubule-interfering agent, in non-small cell lung cancer PC-14 cells and astrocytes. Invest New Drugs 19:293
38. Nerlov C, De Cesare D, Pergola F, Caraccilo A, Blasi F, Johnsen M, Verde P (1992) A regulatory element that mediates co-operation between a PEA3-AP-1 element and AP-1 site is required for phorbol ester induction of urokinase enhancer activity in HepG2 hepatoma cells. EMBO J 11:4573
39. Nihei Y, Suzuki M, Okano A, Tsuji T, Akiyama Y, Tsuruo T, Saito S, Hori K, Sato Y (1999) Evaluation of antivascular and antimitotic effects of tubulin binding agents in solid tumor therapy. Jpn J Cancer Res 90:1387
40. Ohe Y, Podack ER, Olsen KJ, Miyahara Y, Miura K, Saito H, Koishihara Y, Ohsugi Y, Ohira T, Nishio K, Saijo N (1993) Interleukin-6 cDNA transfected Lewis lung carcinoma cells show unaltered net tumor growth rate but cause weight loss and shorten survival in syngenic mice. Br J Cancer 67:939
41. Ohe Y, Podack ER, Olsen KJ, Miyahara Y, Ohira T, Miura K, Nishio K, Saijo N (1993) Combination effect of vaccination with IL2 and IL4 cDNA transfected cells on the induction of a therapeutic immune response against Lewis lung carcinoma cells. Int J Cancer 53:432
42. Ohira T, Ohe Y, Heike Y, Podack ER, Olsen KJ, Nishio K, Nishio M, Miyahara Y, Funatyama Y, Ogasawara H, Arioka

H, Kato H, Saijo N (1994) Gene therapy for Lewis lung carcinoma with tumor necrosis factor and interleukin 2 cDNAs co-transfected subline. Gene Ther 1:269
43. Okamura K, Sato Y, Matsuda T, Hamanaka R, Ono M, Kohno K, Kuwano M (1990) Endogenous basic fibroblast growth factor-dependent induction of collagenase and interleukin-6 in tumor necrosis factor-treated human microvascular endothelial cells. J Biol Chem 226:19162
44. Otani M, Natsume T, Watanabe J, Kobayashi M, Murakoshi M, Mikami T, Nakayama T (2000) TZT-1027, an antimicrotubule agent, attacks tumor vasculature and induces tumor cell death. Jpn J Cancer Res 91:837
45. Salgado R, Vermeulen PB, Benoy I, Weytjens R, Huget P, Van Marck E, Dirix LY (1999) Platelet number and interleukin-6 correlate with VEGF but not with bFGF serum levels of advanced cancer patients. Br J Cancer 80:892
46. Schweigerer L, Malerstein B, Gospodarowicz D (1987) Tumor necrosis factor inhibits the proliferation of cultured capillary endothelial cells. Biochem Biophys Res Commun 143:997
47. Shimomura K, Manda T, Mukumoto S, Kobayashi K, Nakano K, Mori J (1988) Recombinant human tumor necrosis factor-α: thrombus formation is a cause of anti-tumor activity. Int J Cancer 41:243
48. Sleijfer S, Le TK, de Jong S, Timmer-Bosscha H, Withoff S, Mulder NH (1999) Combined cytotoxic effects of tumor necrosis factor-alpha with various cytotoxic agents in tumor cell lines that are drug resistant due to mutated p53. J Immunother 22:48
49. Sugiura K, Stock CC (1955) Studies in a tumor spectrum III. The effect of phosphoramides on the growth of a variety of mouse and rat. Cancer Res 15:38
50. Vandenbunder B, Pardanaud L, Jaffredo T, Mirabel MA, Stehelin D (1989) Complementary patterns of expression of c-ets-1, c-myb and c-myc in the blood-forming system of the chick embryo. Development 106:265
51. Vandenbunder B, Wernert N, Queva C, Desbiens X, Stehelin D (1994) Does the transcription factor c-ets-1 take part in the regulation of angiogenesis and tumor invasion? Folia Biol 40:301
52. Watanabe J, Natsume T, Fujio N, Miyasaka K, Kobayashi M (2000) Induction of apoptosis in human cancer cells by TZT-1027, an antimicrotubule agent. Apoptosis 5:345
53. Zhao E, Zhou M, Fu C, Shen B, Zhang Q, Lian L (1995) Effects of TNF alone or in combination with chemotherapeutic agents on human ovarian cancers in vitro and in nude mice. Chin Med J 108:571